International Journal of Scientific Engineering and Applied Science (IJSEAS) - Volume-2, Issue-1, January 2016
ISSN: 2395-3470
www.ijseas.com

PI Controller Based Bidirectional Soft Switched Converter for Motor Drive Applications

[1]Stalin. B, [2]Dr. Sivakumaran. T.S.
[1]Research Scholar (PT), Faculty of Electrical Engineering, Anna University, Chennai. 600025, India
[2]Professor & Dean PG Studies, Arunai College of Engineering, Tiruvannamalai, India

Abstract

In recent years bidirectional dc to dc converters are widely used in electric vehicles. In electric vehicles the energy is transferred between battery and motor drive and also the battery acts as a catalyst to provide energy boost. But due to its short driving range and high cost has limited its use. Hence a bidirectional converter is required to control Power flow in both motoring and regenerative braking operation so that the overall drive system efficiency increases significantly. This paper presents a closed loop bidirectional converter with a PI controller for a motor drive system. In order to reduce the losses and to increase the conversion efficiency of the proposed converter all the switches are turned OFF and turned ON at zero current and zero voltage crossing, so the proposed converter act as Zero Current Transient buck to charge the battery and Zero Voltage Transient boost to discharge the battery. The output voltage is maintained constant even with varied input voltage using a PI controller. The proposed topology is verified through simulations using MATLAB/Simulink and the output performances are analyzed.

Key words: *Closed loop control, PI controller, Zero Voltage Transient (ZVT), Zero Current Transient (ZCT), Bidirectional Converter, Battery, Separately excited DC motor.*

1. Introduction

In soft switching based storage system, the efficiency of system is depends on the size and cost; it can be increased by a combination of batteries or ultra capacitors. Also, the leakage current of ultra capacitor is high so the voltage imbalance problem has to be occurred. The development of high power bi-directional DC-DC converters has become an important topic because of the requirement in energy storage systems. Battery fed electric vehicles are commonly being used for EV applications due to zero emission, guaranteed load leveling, good transient operation and energy recovery during braking operation. Hence converter with bidirectional power flow capabilities is required to connect the battery to the DC motor drive system [2]. The output voltage should not be maintained constant with variation in input voltage in open loop system hence a closed loop system is required [1]. A PI controller based closed loop system is used for controlling the switching pulses so that the output voltage is maintain constant with variation in input voltage [3]. A fractional order PID controller is used to control auxiliary switch so that the efficiency of the converter with soft switching has been increased. An Artificial Intelligence technique is used to tune PI controller (Improved Particle Swarm Optimization algorithms) [4]. In DC distributed power systems PI controllers are not only dampers the bus transients but also keeps the storage voltage level [5]. The energy management system in Hybrid Electric Vehicle is maintained and controlled by using PI controller during charging and discharging of the battery [6]. There are many construction types of power system of multi energy Electric Vehicles such as Fuel Cells + Auxiliary Power Battery+ Ultra Capacitor, Fuel Cells + Ultra Capacitor, Fuel Cells + Power Battery, Power Battery + Ultra Capacitor. Measure and control circuit detects the voltage of power battery and ultra capacitor to determine the work status of the Ultra Capacitor [8]. A hybrid power source with batteries and super Capacitors gives the power in steady state during transient state [9]. An Ultra Capacitor system for an electric vehicle is used to allow higher acceleration and decelerations of the vehicle with minimal loss of energy and minimal degradation of the main battery [10]. The features of of Zero Voltage Switching ensures the high operating frequency, high step-up ratio, low voltage stress across the switches and increase the conversion efficiency of the converter[7]. A resonant network in parallel with the switches achieves Zero Voltage Switching for both active and passive switches without increasing their voltage and current stresses [11]. A Zero Current Transient (ZCT) implement ZCS turn OFF for the

International Journal of Scientific Engineering and Applied Science (IJSEAS) - Volume-2, Issue-1, January 2016
ISSN: 2395-3470
www.ijseas.com

transistors without substantially increases in voltage or current stresses in the switches [12]. ZCT PWM FB dc/dc converter not only achieves zero current switching for all switches in the entire load ranges but it also realizes soft commutation for the output rectifier diode. Further the auxiliary circuit also helps to turn on the main switches softly [13]. ZCZVT PWM boost converter differ from a hard switching PWM boost converter by the presence of an additional shunt resonant network formed by two resonant capacitors C_{R1} and $C_{R2,}$ a resonant inductor L_R a bidirectional auxiliary switch and two auxiliary diodes to provide ZCS and ZVS at both turn ON and turn OFF for the main switch [14]. The ZVT principle is based on the auxiliary circuit carrying higher current than the steady state boost current for a fraction of the switching cycle to achieve soft switching for the switches and diodes used in the converter. So ZVT converters have more conduction losses than the hard switched boost converters but still have higher efficiencies due to reduced switching losses [15].

Generally DC motor drives are categorized in to non-regenerative and regenerative in industry. Non regenerative is
normal conventional type, used to control speed and torque in one direction whereas regenerative DC drives are four quadrant drives, not only controlling speed and direction of rotation but also direction of motor torque. This paper is based on regenerative DC drive type with a closed loop system implementing a PI controller to maintain constant output voltage with variation in input voltage. The proposed topology is preferred for maintaining the conversion efficiency and its operating modes are analyzed by the equivalent circuit models during both buck and boost mode of conversion.

2. Proposed Circuit and Operation

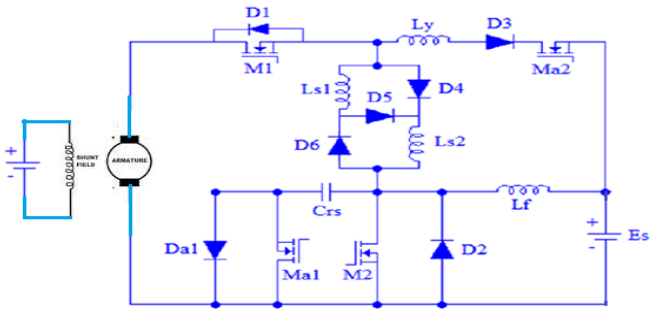

Fig.1. Structure of the proposed circuit

The proposed circuit is shown in Figure. 1, which consists of an auxiliary switch between the battery and separately excited DC motor, which improves the conversion ratio and reduces the leakage current of inductor while charging and discharging. The proposed circuit is operated in two modes such as buck mode and the boost mode. During the buck mode of operation the switch M_1 and the diode $D_2$is ON and the circuit act as ZCT buck to charge the battery. Similarly for the boost mode of operation the switch M_2 and the diode D_1 is ON and the circuit act as ZVT boost to discharge the battery. The auxillary switches M_{a1} and M_{a2}, along with the switched inductors (L_{s1} and L_{s2}) and diodes (D_4, D_5 and D_6) will improve the voltage gain of the system. The auxiliary inductor L_y and resonant capacitors C_{rs} are utilized to achieve soft switching.

2.1 Buck Mode Of Operation

During this mode diode D_2 and the switch M_1 is turned ON, the circuit act as a ZCT buck to charge the battery. In this mode input voltage and inductor L_f current are assumed as constant. Similarly all the components present in the circuit considered to be ideal. The one switching cycle consists of six modes of operation which is shown in following figure 2.

Mode 1:(t_0 –t_1)

At the starting time of the mode 1 operation is t_0 to t_1, during this time the diode D_2 and the switch M_1 is turned ON. The output current I_{out} is flowing through the diode D_2, the switch is turned ON with the ZCS to charge an ultra capacitor. At the end of the mode the time is t_1, in this period the switched inductor current is reaches to the output current I_{out}. The voltage equation of the mode 1 is given in the following equation (1).

$$E_{low} = \sum_{\substack{i=1 \\ j=1}}^{n} L_{sj}\frac{dI_j}{dt} + \sum_{j=1}^{n}\frac{kT_j}{q} + L_f\frac{dI_f}{dt} + nV_T \ln\left[\frac{I_{out}}{I_s}\right]_{D2} + \sum_{j=1}^{n} I_{out}R_a \quad (1)$$

The output current across the diode D_2 is given in the following equation (2)

$$I_{out} = \frac{E_s}{SL} \quad (2)$$

The current of the switched inductor is defined by the following equation (3)

$$I_{SL} = E_s\left(\frac{1}{(L_{s1}+L_{s2})}\right) + I_{s5}(e^{V_d/(nV_T)} - 1) \quad (3)$$

Where K is the Boltzmann constant, T absolute temperature, q magnitude of the charge, is the ideality

International Journal of Scientific Engineering and Applied Science (IJSEAS) - Volume-2, Issue-1, January 2016
ISSN: 2395-3470
www.ijseas.com

factor, I_{s5} is the saturation current of the diode 5, V_d is the voltage across the diode, L_{s1} and L_{s2} are the switched inductors, V_T is the thermal voltage of the diode, E_s is the supply voltage, I_{out} is the output current and SL is the switched inductor.

Mode 2: $(t_1 - t_2)$

During this mode of operation current of the main switch reaches to zero at $t = t_1$ and the diode D_2 is turned OFF, i.e., soft switching turn OFF ZCZVS. The resonance of the switched inductors (L_{s1} and L_{s2}) and capacitors C_{rs} start flows through the diode D_{a1}. The resonant condition components current and the voltage of the mode 2 are given in the following equations.

$$E_{low} = \sum_{\substack{i=1 \\ j=1}}^{n} L_{sj} \frac{dI_j}{dt} + \frac{kT_1}{q} + L_f \frac{dI_f}{dt} + nV_T \ln\left[\frac{I_{out}}{I_s}\right]_{Da1} + \frac{1}{C_{rs}} \int i_{rs}(t)dt + \sum_{j=1}^{n} I_{out}(R_a) \quad (4)$$

The output current and the capacitor voltage of this mode are given in the following equations (5) and (6).

$$I_{out}(t_2) = I_{SL} - E_s\left[\frac{1}{Z_{SLC}} \sin(\omega_{SLC}(t_2))\right] \quad (5)$$

$$E_{Crs}(t_2) = E_s[1 - \cos(\omega_{SLC}(t_2))] \quad (6)$$

Where, $\omega_{SLC} = \frac{1}{\sqrt{(L_{s1} + L_{s2})C_{rs}}}$ and $Z_{SLC} = \sqrt{\frac{L_{s1} + L_{s2}}{C_{rs}}}$

Mode 3: $(t_2 - t_3)$

During this mode of operation resonant capacitor current reaches to zero at $t = t_2$. The auxiliary switch M_{a1} is turned off, so the resonance of the inductor and capacitor is stopped. This mode of operation the resonant capacitor C_{rs} voltage reaches $2E_s$ and the switched inductor current reaches to the output current I_{out}.

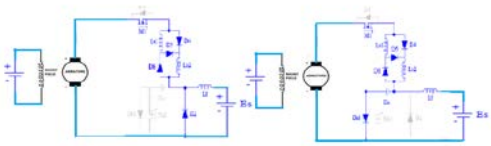

Mode 1 Mode 2

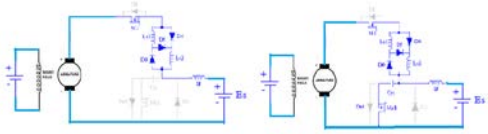

Mode 3 Mode 4

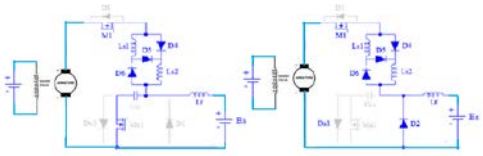

Mode 5 Mode 6

Fig.2. Buck Modes of Operation

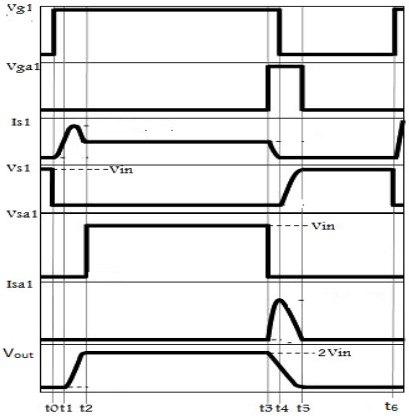

Fig.3. Waveforms for Buck Operation

The power flows from the source input to the output enhanced ultra capacitor. The voltage of the mode is given by the following equation (7).

$$E_{low} = \sum_{\substack{i=1 \\ j=1}}^{n} L_{sj} \frac{dI_j}{dt} + \frac{kT_1}{q} + L_f \frac{dI_f}{dt} + \sum_{j=1}^{n} I_{out}(R_a) \quad (7)$$

Mode 4: $(t_3 - t_4)$

During this mode of operation the auxiliary switchM_{a1} is turned off under ZCS condition at time t_3. In this mode the resonance between the resonant capacitor and the switched inductor starts, so that the switched inductor fully discharge i.e., it reaches zero. At the end of the mode operation 4, the switchM_1 softly turned OFF at ZCS. The voltage equation of this mode is given in the following equation (8).

$$E_{low} = \sum_{\substack{i=1 \\ j=1}}^{n} L_{sj} \frac{dI_j}{dt} + \sum_{j=1}^{n} \frac{kT_j}{q} + L_f \frac{dI_f}{dt} + \frac{1}{C_{rs}} \int I_{rs}(t)dt + \sum_{j=1}^{n} I_{out}(R_a) \quad (8)$$

The output current of this mode can be described as the following equation (9)

$$I_{out}(t_4) = I_{SL} + E_s\left[\frac{1}{Z_{SLC}} \sin(\omega_{SLC}(t_4))\right] \quad (9)$$

$$E_{Crs}(t_4) = E_s[1 + \cos(\omega_{SLC}(t_4))] \quad (10)$$

$$\bar{I}_{out} \leq \frac{E_s}{Z_{SLC}} \quad (11)$$

When the switched inductor current I_{sL} reaches zero, the ZCS condition occurs for switch M_1. The equation 10 shows the resonant capacitor C_{rs} voltage at the mode 4 operation. The above equation 11 is the constraint for ZVS, if the output current is less than the condition, i.e., $\bar{I}_{out} < \frac{E_s}{Z_{SLC}}$, additional one mode is added to the buck operation and also the body diode of the main switch is conduct.

Mode 5: $(t_4 - t_5))$

This mode started at t_4, in which the switched inductor current I_{SL} fully decreases to zero and the output current flows through the resonant capacitor C_{rs}. So the resonance voltage decreases, at the end of this mode, the resonant capacitor voltage reaches zero. The voltage of this mode is given in the following equation (12).

$$E_{low} = \frac{1}{C_{rs}}\int I_{rs}(t)dt + \frac{kT_{a1}}{q} + L_f\frac{dI_{out}}{dt} + \sum_{j=1}^{n} I_{out}(R_a) \quad (12)$$

Mode 6:$(t_5 - t_6)$

At the starting of this mode t_5 the resonant capacitor C_{rs} voltage reduced to zero, so the diode D_2 is turned ON under the soft switching ZVS condition. In this mode the auxiliary switch $M_{a1}$is turned OFF under the ZVS condition and the energy flows from the inductor L_f to the battery. In this condition the voltage of this mode is given by the following equation (13).

$$E_{low} = nV_T \ln\left[\frac{I_{out}}{I_s}\right]_{D2} + L_f\frac{dI_{out}}{dt} + \sum_{j=1}^{n} I_{out}(R_a) \quad (13)$$

The above six modes are completed in one switching cycle, i.e., one switching cycle have six modes of operation.

2.2 Boost Mode Of Operation

During this boost mode of operation diode D_1 and the switch M_2 is turned ON and the circuit act as a ZVT boost to discharge the battery. In this mode of operation, circuit input voltage and the inductor L_f current are assumed as constant. Similarly all the components present in the circuit considered to be an ideal condition. The one switching cycle consists of eight modes of operation which is shown in following fig. 4.

Mode 1: $(t_0 - t_1)$

At this mode of operation starting at t_0, during this time the diode D_1 is turned ON, the current flows through the inductor L_f. In this time the auxiliary switches M_{a1} and M_{a2} is turned ON, due to this the auxiliary inductor L_y voltage is E_s -E_b and causes the current of the inductor to increase. At the end of this mode the auxiliary inductor current I_{Ly} reaches the output current I_{out}.

The voltage equation of this mode can be described in equation (14).

$$E_{high} = \sum_{j=1}^{n} I_{out}R_a + \sum_{\substack{i=1\\ j=1}}^{n}(L_{sj} + L_f)\frac{dI_j}{dt} + \frac{1}{C_{rs}}\int I_{rs}(t)dt + \sum_{j=1}^{n}\frac{kT_j}{q} + L_y\frac{dI_{out}}{dt} + \sum_{j=1}^{n} nV_T \ln\left[\frac{I_{out}}{I_s}\right]_{Dj} \quad (14)$$

The output current of the circuit is given by the following equation (15)

$$I_{out} = \frac{E_s - E_b}{I_{Ly}}, \quad (15)$$

Mode 2:$(t_1$-$t_2)$

This mode of operation starts at time t_1, in this time the auxiliary inductor L_y current decreases to zero. During this condition the resonant capacitor C_{rs} voltage is $E_s + Z_{SLC}\ I_{out}$. The auxiliary switches M_{a1} and M_{a2} turned ON under the soft switching ZCS and resonance between the resonant capacitor C_{rs}, auxiliary inductor L_y and switched inductor SL flow through these auxiliary switches. At the end of this mode the resonant capacitor C_{rs} voltage reaches zero. The voltage equation of this mode is given by the following equation (16).

$$E_{high} = \sum_{j=1}^{n} I_{out}R_a + \sum_{\substack{i=1\\ j=1}}^{n}(L_{sj} + L_f + L_y)\frac{dI_j}{dt} + \frac{1}{C_{rs}}\int I_{rs}(t)dt + \sum_{j=1}^{n}\frac{kT_j}{q} + \sum_{j=1}^{n} nV_T \ln\left[\frac{I_{out}}{I_s}\right]_{Dj} \quad (16)$$

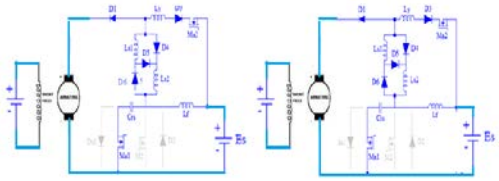

Mode 1 Mode 2

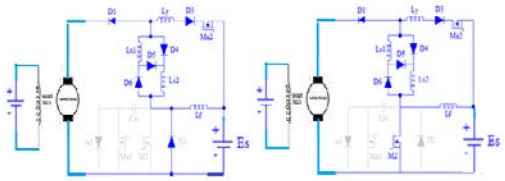

International Journal of Scientific Engineering and Applied Science (IJSEAS) - Volume-2, Issue-1, January 2016
ISSN: 2395-3470
www.ijseas.com

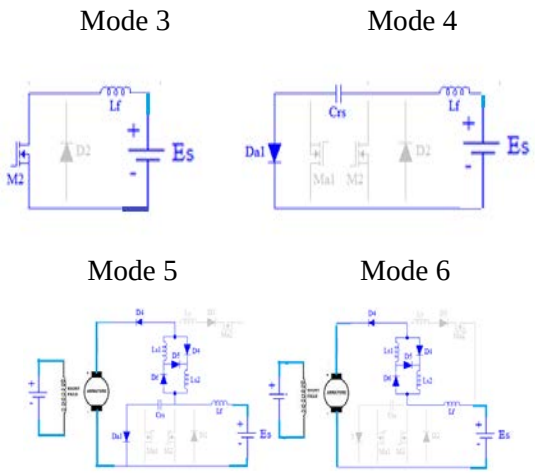

Fig.4. Boost Modes of operation

The output current and the voltage across the resonant capacitor are given in the following equations (17) and (18).

$$I_{out}(t_2) = I_{SL}(t_2) - \frac{E_s + Z_{SLC} I_{out} - \sum_{i=1}^{n} E_{low}}{Z_{SLY}} \sin(\omega_{SLY}(t_2)) \quad (17)$$

$$E_{crs} = \left(E_s + Z_{SLC} - \sum_{i=1}^{n} E_{low} \right) \cos(\omega_{SLY}(t_2)) + \sum_{i=1}^{n} E_{low} \quad (18)$$

Where, $\omega_{SLY} = \frac{1}{\sqrt{C_{rs}(L_{s1} + L_{s2} + L_y)}}$ and $Z_{SLY} = \sqrt{\frac{L_{s1} + L_{s2} + L_y}{C_{rs}}}$

Mode 3 :($t_2 - t_3$)

During this mode of operation starts at t_2, the resonant capacitor C_{rs} is completely discharge due to the resonance cycle. At this time diode D_2 conducts and the switched inductor SL current reaches the output current I_{out}. At the end of this mode of operation switch M_2 is turned ON under soft switched ZCS condition.

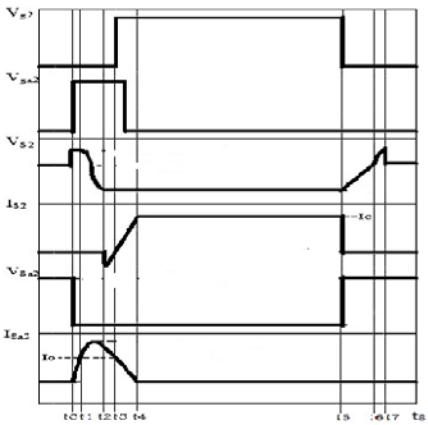

Fig.5. Waveforms for Boost Operation

The voltage equation of this mode is given in the following equation (19).

$$E_{high} = \sum_{j=1}^{n} I_{out} R_a + \sum_{\substack{i=1 \\ j=1}}^{n} (L_{sj} + L_f + L_y) \frac{dI_j}{dt} + \frac{kT_{a2}}{q} + \sum_{j=1}^{n} nV_T \ln\left[\frac{I_{out}}{I_s} \right]_{Dj} \quad (19)$$

The output current of this mode can be described as the following equation (20)

$$I_{out}(t_3) = I_{SL}(t_3) - \frac{E_s + Z_{SLC} I_{out} - \sum_{i=1}^{n} E_{low}}{Z_{SLY}} \left[1 - \left(\frac{\sum_{i=1}^{n} E_{low}}{E_s + Z_{SLC} I_{out} - \sum_{i=1}^{n} E_{low}} \right) \right]^{1/2} - \frac{\sum_{i=1}^{n} E_{low}}{L_{s1} + L_{s2} + L_y} (t_2) \quad (20)$$

Mode 4: (t_3-t_4)

This mode of operation starts at t_3, during this time the switched inductor SL current decreases from the output current I_{out}. The switch current I_{M2} increases linearly and at the end of this mode the switch current I_{M2} reaches to the output current I_{out} at t_4. The voltage equation of this mode equation is given in the following equation (21) and output current is given in the equation (22)

$$E_{high} = \sum_{j=1}^{n} I_{out}(R_a) + \sum_{\substack{i=1 \\ j=1}}^{n} (L_{sj} + L_f + L_y) \frac{dI_j}{dt} + \sum_{j=1}^{n} \frac{kT_j}{q} + \sum_{j=1}^{n} nV_T \ln\left[\frac{I_{out}}{I_s} \right]_{Dj} \quad (21)$$

$$I_{out}(t_4) = I_{SL}(t_4) + \frac{\sum_{i=1}^{n} E_{uci}}{L_{s1} + L_{s2} + L_y} (t_4) \quad (22)$$

Mode 5: ($t_4 - t_5$)

During this mode of operation the auxiliary switches are turned ON and the energy flows from the battery to

International Journal of Scientific Engineering and Applied Science (IJSEAS) - Volume-2, Issue-1, January 2016
ISSN: 2395-3470
www.ijseas.com

the inductor L_f. The voltage of this mode of operation is given in the following equation (23).

$$E_{high} = \sum_{j=1}^{n} I_{out}(R_a) + L_f \frac{dI_f}{dt} + \sum_{j=1}^{n} \frac{kT_j}{q} \quad (23)$$

Mode 6 :(t_5 –t_6)

This mode of operation the switch is turned OFF, the inductor L_f current flows through the resonant capacitor C_{rs}, the resonant capacitor is charged by the current and voltage E_s. Due to this condition the switch is turned OFF under the ZVS condition. The equivalent circuit of this mode is shown in the fig.3. The voltage of the equivalent circuit is given in the following equation (24).

$$E_{high} = \sum_{j=1}^{n} I_{out}(R_a) + L_f \frac{dI_f}{dt} + \frac{1}{C_{rs}} \int I_{rs}(t)dt + nV_T \ln\left[\frac{I_{out}}{I_s}\right]_{Da1} \quad (24)$$

The output current of this mode of operation can be described as the following equation (25).

$$I_{out}(t_6) = E_{crs}(t_6) * C_{rs}(t_6) \quad (25)$$

Mode 7 : ($t_6 - t_7$)

At the starting time of this mode is t_6, the capacitor voltage reaches to E_s. During this time the diode D_1 starts to conduct and the diode current increases due to the switched inductor SL. At the end of this mode of operation, the capacitor voltage reaches $E_s + Z_{SLC}\, I_{out}$. The voltage equation of this mode of operation is given in the following equation (26).

$$E_{high} = \sum_{j=1}^{n} I_{out}(R_a) + \sum_{\substack{i=1 \\ j=1}}^{n} (L_{sj} + L_f) \frac{dI_j}{dt} + \frac{1}{C_{rs}} \int I_{rs}(t)dt + \sum_{j=1}^{n} nV_T \ln\left[\frac{I_{out}}{I_s}\right]_{Daj} \quad (26)$$

Mode 8 :($t_7 - t_8$)

During this mode of operation the energy flows from the battery because the resonant capacitor is overcharged and the auxiliary switch M_{a1} is turned off under ZCS. At this condition the switched inductor current reaches to the output current I_{out}. The voltage equation of this mode is given in the following equation (27).

$$E_{high} = \sum_{j=1}^{n} I_{out}(R_a) + \sum_{\substack{i=1 \\ j=1}}^{n} (L_{sj} + L_f) \frac{dI_j}{dt} + nV_T \ln\left[\frac{I_{out}}{I_s}\right]_{D1} \quad (27)$$

3. PI Controller for DC to DC Converter

PI controllers are mostly implemented in bidirectional converters due its simplicity and ability to tune a few parameters automatically and less overshoot and small settling time can be obtained. PI controllers can be used to solve even a very complex control problem, especially when combined with different blocks.

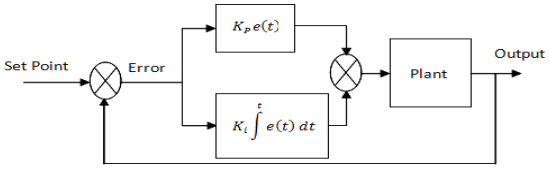

Fig. 6. Structure of PI Controller

The structure of PI controller is shown in fig.6. It is a combination of proportional (P) and Integral (I) parameters, the proportional (P) part are used to set a desired set-point, while the integral part (I) is used to account the accumulation of past errors and rate of change of error in the process respectively.

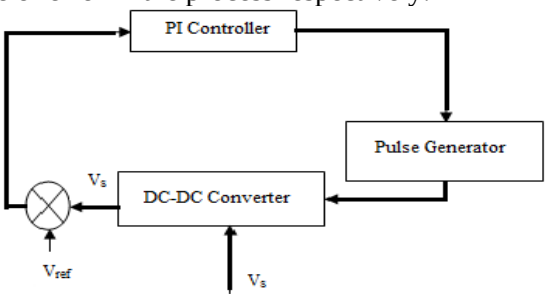

Fig.7.Block diagram of PI Controller for DC to DC Converter

In control techniques, as K_p increased the system speed increase and the steady state error decreases but is not eliminated, as K_i increases, the steady state error goes to zero and the system tends towards instability. So Proportional and Integral controllers are never used alone.

As Proportional control, $P(t) = K_p\, e(t)$. Proportional control P(t), where the signal is proportional to the error signal. As Integral control, $i(t) = K_i \int e(t)\, dt$. Integral control i(t), where the signal is proportional to the cumulative values of error signal, where K_p and K_i are constants.

The overall control of PI controller is

$$PI(t) = K_p\, e(t) + K_i \int e(t)\, dt.$$

In S – domain,

$$PI(S) = [\, K_p + K_i / S]\, E(s)$$

4. Results and Discussions

International Journal of Scientific Engineering and Applied Science (IJSEAS) - Volume-2, Issue-1, January 2016
ISSN: 2395-3470
www.ijseas.com

The proposed circuit is simulated in MATLAB/Simulink platform. The simulation model for buck and boost operation with PI compensator are shown in Fig. 8 and 9 respectively and the simulated result waveforms for both buck and boost operation are shown in Fig.10 and Fig. 11 respectively. The proposed circuit with PI controller is validated by injecting a disturbance in the input voltage and the impact of this disturbance in the output is corrected by tuning the PI controller which is shown in the Fig. 10 and 11 for both the modes of operation.

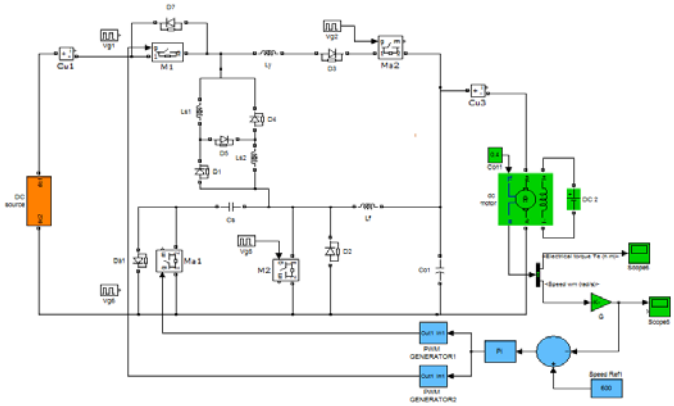

Fig.8. Buck operation of the proposed circuit

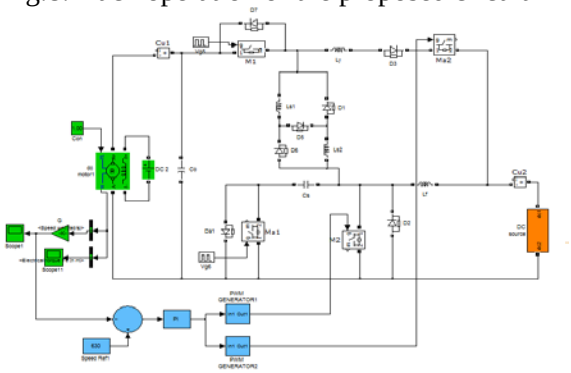

Fig.9. Boost operation of the proposed circuit

4.1 Results for Buck Operation

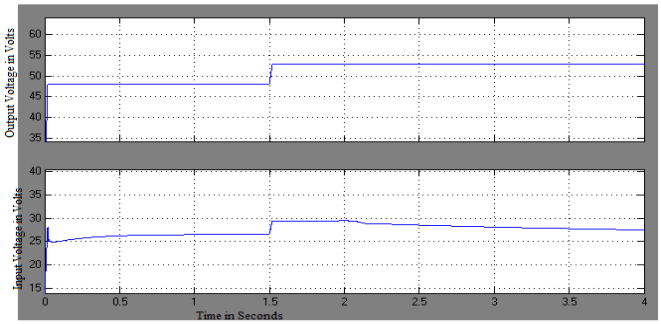

(a) Input Voltage and Output Voltage

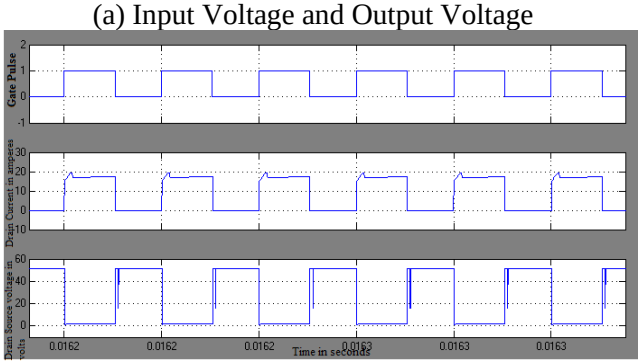

(b) Gate pulses, drain current and drain source voltage across switch M_1

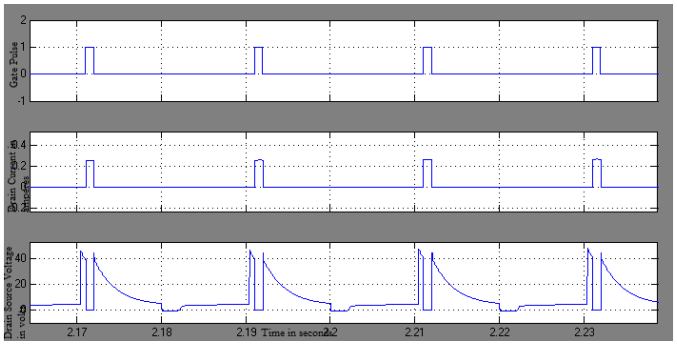

(c) Gate pulses, drain current and drain source voltage across switch M_{a1}

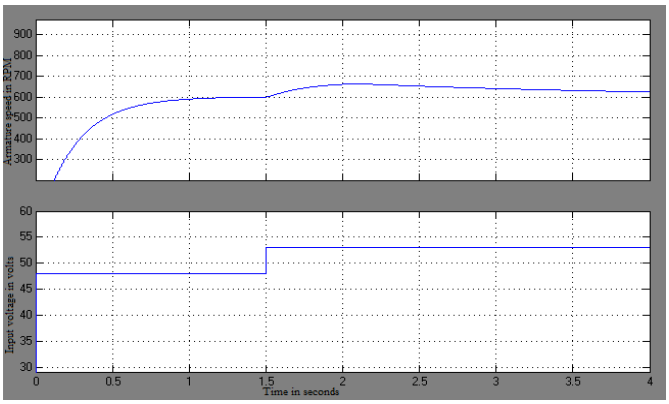

(d) Armature speed in rpm and Input voltage

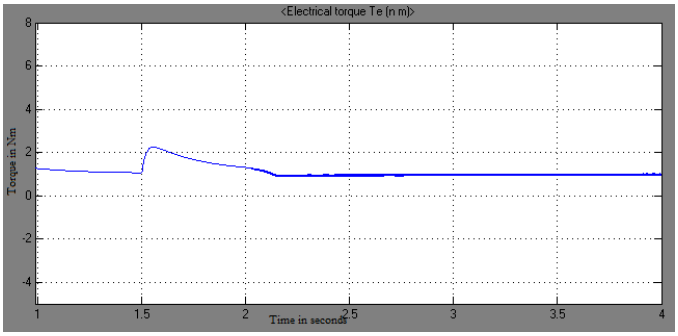

(e) Torque

Fig.10. Waveforms for buck operation of the proposed circuit

4.2 Results for Boost Operation

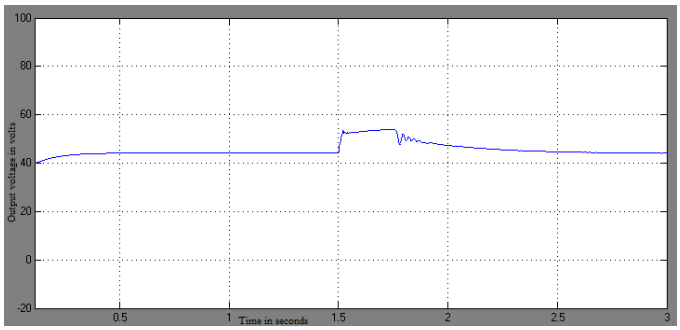

(a) Output Voltage

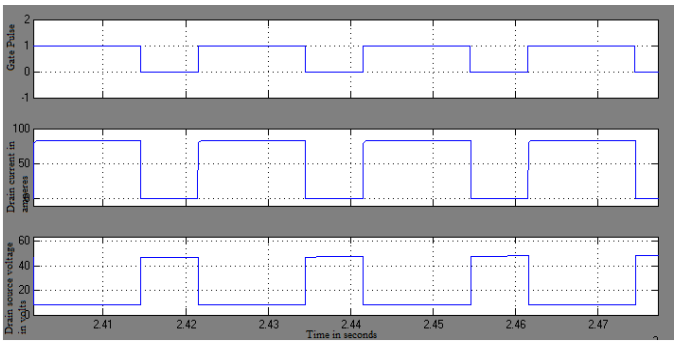

(b) Gate pulses, drain current and drain source voltage across switch M_2

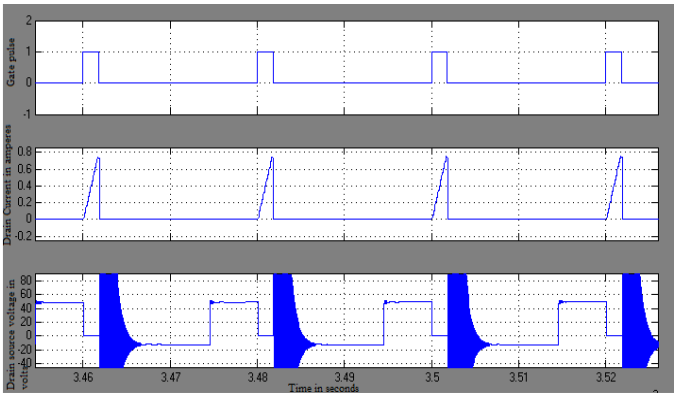

(c) Gate pulses, drain current and drain source voltage across switch M_{a2}

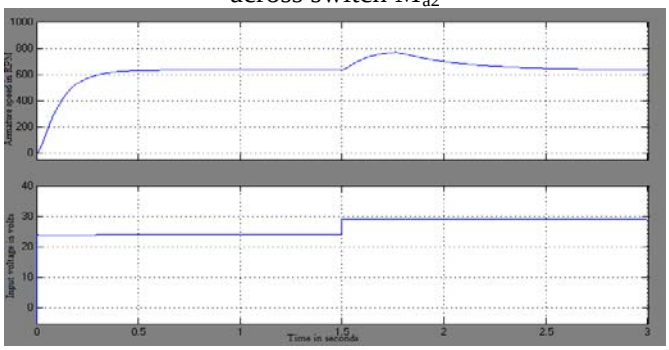

(d) Armature speed in rpm and input voltage

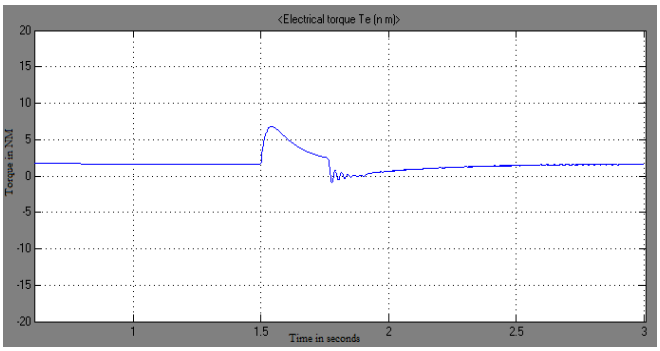

(e) Torque

Fig.11. Waveforms for boost operation of the proposed circuit

4.3 Results Discussion

The response of the proposed closed loop circuit with PI controller for buck and boost operation are shown in Fig. 10 & 11 respectively. The output voltage during both buck and boost operation is sensed and compare with reference voltage, the error is applied to a PI controller and corrected which is shown in Fig. 10 (a) and Fig 11. (a) respectively. From the waveforms it can be seen that the output voltage gets disturbs, oscillates and settles to the reference value. Similarly the armature speed and torque of the motor corresponding to the input voltage for both the operating modes are shown in Fig. 10 (d), (e) and Fig. 11(d), (e) respectively. The main and auxiliary switches M1, M2, Ma1and Ma2 are turned ON and OFF at zero crossing for both the modes of operation are shown in Fig. 10 (b), (c) and Fig. 11(b), (c) respectively, from the corresponding waveforms it can be seen that soft switching is achieved for all the switches of the proposed circuit.

5. Conclusion

In this paper closed loop PI controlled bidirectional soft switching converter is proposed and its responses were analyzed and described with corresponding waveforms. ZCT and ZVT techniques are applied to achieve soft switching for main and auxiliary switches, in order to increase the converter voltage conversion efficiency, but the settling time of the waveforms after error correction is little more and this can be reduced by fine tuning of PI controller. The performance of proposed circuit may be analyzed with other Artificial Intelligence controllers and compared for better performance in the future.

References

[1] S. Preethi1, Mahendiravarman, A. Ragavendiran and M. Arunprakash, “Matlab /Simlink based closed Loop Control of Bi-Directional DC – DC Converter” International Journal of Engineering Science and Innovative Technology (IJESIT), Vol. 3, Issue 5, September 2014.

[2] Premananda Pany, R.K. Singh and R.K. Tripathi, “Bidirectional DC-DC Converter fed drive for electric vehicle system”, International Journal of Engineering, Science and Technology, Vol. 3, No. 3, 2011, pp.101-110.

[3] Atul Kumar and Prerna Gaur, “Operation of DC/DC Converter fro Hybrid Electric Vehicle”, International journal of Electronic and Electrical Engineering, Vol.7, No.4, 2014.

[4] K. Giridharan and A. Karthikeyan,“Fractional Order PID Controller Based Bidirectional DC/DC Converter”, International Journal Of Innovative Research in Science, Engineering and Technology, Vol.3, Issue 3, 2014.

[5] Joonmin Lee, Bong Jun Seok, Jae Du La and Young Seok Kim, “A Design of a PI Compensator for a Bidirectional DC-DC Converter in a DC Distributed Power System”, Journal of International Conference on Electrical Machines and Systems, Vol. 1, No. 3, pp.391-396, 2012.

[6] S. Saravanan and G. Sugumaran, “Energy Management System in HEV Using PI Controller”, International Journal of Electrical, Computer, Electronics and Communication Engineering, Vol. 8, No . 2, 2014.

[7] R. Sudha amd P.M. Dhanasekaran, “DC-DC Converters Using PID Controller and Pulse Width Modulation Technique”, International Journal of Engineering Trends and Technology(IJETT), Vol. 7, No.4, 2014.

[8] Lianbing Li, Lining Sun, Zuojun and Hexu Sun, “ Ultracapacitor Control Strategy of EV with Energy Hybridization”, IEE Vehicle Power and Propulsion Conference (VPPC), September 3-5, 2008, Harbin, China.

[9] Sebastien Wasterlain, Alcicek Guven, Hamid Gualous, Jean Francois Fauvarque and Roland Gallay, “Hybrid power source with batteries and supercapacitor for vehicle applications”.

[10] Jaun W. Dixon and Micah E. Ortuzar, "Ultracapacitors+ DC-DC Converters in Regenerative Braking System", IEEE AESS Systems Magazine, August 2002.
[11] Guichao Hua, Ching-Shan Leu, Yimin Jiang and Fred C. Y. Lee, "Novel Zero- Voltage-Transition PWM Converters", IEEE Transactions on Power Electronics, Vol. 9, No. 2, March 1994.
[12] Guichao Hua, Eric X. Yang, Yimin Jiang and Fred C. Lee, "Novel Zero- Voltage-Transition PWM Converters", 0-7803-1243-0/93$03.00 © 1993 IEEE.
[13] Junming Zhang, Xiaogao Xie, Xinke Wu, Guoliang Wu and Zhaoming Qian, "A Novel Zero-Current- Transition Full Bridge DC/DC Converter", IEEE Transactions on Power Electronics, Vol. 21, No. 2, March 2006.
[14] Carlos Marcelo de Oliveira Stein, "A True ZCZVT Commutation Cell for PWM Converters", IEEE Transactions on Power Electronics, Vol. 15, No. 1, January 2000.
[15] Nikhil Jain, Praveen K. Jain and Geza Joos, "A Zero Voltage Transition Boost Converter Employing a Soft Switching Auxiliary Circuit with Reduced Conduction Losses", IEEE Transactions on Power Electronics, Vol. 19, No. 1, January 2004.

Author Information

B. Stalin obtained his Bachelor's degree in Electrical and Electronics Engineering from University of Madras in 2002. Then he obtained his Master's degree in Power Electronics and Industrial Drives from Sathyabama University, Chennai, and Tamilnadu in 2010. Now he is doing his research in Electrical Engineering from Anna University Chennai. Currently he is working as an Associate Professor in the Department of Electrical and Electronics Engineering at Gopal Ramalingam Memorial Engineering College, Chennai. He is Graduate Student Member of IEEE for 5 years.

T.S.Sivakumaran was born in Panruti, India, on December 18, 1969. He has obtained B.E (Electrical and Electronics) and M.Tech (Power Electronics) in 1998 and 2002 respectively from Annamalai University and VIT University, Vellore and then Ph.D. in Power Electronics from Annamalai University, Chidambaram in 2009. He is currently Dean (PG studies) in Department of Electrical and Electronics Engineering, Arunai College of Engineering, Tiruvannamalai, India. His research papers (35) have been presented at IEEE / International Conferences in Hong Kong, India, Singapore, SriLanka, Malaysia and Korea. He has two and ten publications in National and International journals. He is a life member of Institution of Engineers (India), Indian Society for Technical Education and IEEE member.